AL/OE-TR-1993-0099

OCULAR DAMAGE INDUCED BY ULTRASHORT LASER PULSES

Joseph A. Zuclich
W. Rowe Elliott
Clarence P. Cain
Gary D. Noojin

KRUG Life Sciences Inc.
San Antonio, Texas

W. P. Roach
Benjamin A. Rockwell

Optical Radiation Division
Brooks Air Force Base, Texas

Cynthia A. Toth

Wilford Hall Medical Center
Lackland Air Force Base, Texas

OCCUPATIONAL AND ENVIRONMENTAL HEALTH DIRECTORATE
8111 18th Street
Brooks Air Force Base, TX 78235-5215

September 1993

Interim Technical Report for Period February 1992 - July 1992

AIR FORCE MATERIEL COMMAND
BROOKS AIR FORCE BASE, TEXAS

ARMSTRONG LABORATORY

NOTICES

When Government drawings, specifications, or other data are used for any purpose other than in connection with a definitely Government-related procurement, the United States Government incurs no responsibility or any obligation whatsoever. The fact that the Government may have formulated or in any way supplied the said drawings, specifications, or other data, is not to be regarded by implication, or otherwise in any manner construed, as licensing the holder, or any other person or corporation; or as conveying any rights or permission to manufacture, use, or sell any patented invention that may in any way be related thereto.

The animals involved in this study were procured, maintained, and used in accordance with the Animal Welfare Act and the "Guide for the Care and Use of Laboratory Animals" prepared by the Institute of Laboratory Animal Resources - National Research Council.

The Office of Public Affairs has reviewed this report, and it is releasable to the National Technical Information Service, where it will be available to the general public, including foreign nationals.

This report has been reviewed and is approved for publication.

Robert M Cartledge

ROBERT M. CARTLEDGE, Lt Col, USAF, BSC
Chief, Optical Radiation Division

REPORT DOCUMENTATION PAGE

Form Approved
OMB No. 0704-0188

1. AGENCY USE ONLY *(Leave blank)*	2. REPORT DATE	3. REPORT TYPE AND DATES COVERED
	September 1993	Interim - Feb 92 - Jul 92

4. TITLE AND SUBTITLE

Ocular Damage Induced by Ultrashort Laser Pulses

5. FUNDING NUMBERS

C - F33615-92-C-0017
PE - 62202F
PR - 7757
TA - 02
WU - 99

6. AUTHOR(S)

Joseph A. Zuclich, W. Rowe Elliott, Clarence P. Cain, Gary D. Noojin, W.P. Roach, Benjamin A. Rockwell, and Cynthia A. Toth

7. PERFORMING ORGANIZATION NAME(S) AND ADDRESS(ES)

The Analytic Sciences Corporation (TASC)
750 East Mulberry Avenue, Suite 302
San Antonio, TX 78212

8. PERFORMING ORGANIZATION REPORT NUMBER

9. SPONSORING/MONITORING AGENCY NAME(S) AND ADDRESS(ES)

Armstrong Laboratory (AFMC)
Occupational and Environmental Health Directorate
8111 18th Street
Brooks Air Force Base, TX 78235-5215

10. SPONSORING/MONITORING AGENCY REPORT NUMBER

AL/OE-TR-1993-0099

11. SUPPLEMENTARY NOTES

Armstrong Laboratory Technical Monitor: Lt Col Robert M. Cartledge, (210) 536-3622.

12a. DISTRIBUTION/AVAILABILITY STATEMENT

Approved for public release; distribution is unlimited.

12b. DISTRIBUTION CODE

13. ABSTRACT *(Maximum 200 words)*

A study has been conducted of interaction effects and damage mechanisms of ultrashort laser pulses in the eye. The preliminary results reported here utilized rabbit subjects and ocular tissues isolated from the rabbit eye. Pulsewidths ranged from 4 ns down to 90 fs. In every case, a visible wavelength was used--either doubled Nd:YAG at 532 nm or the 580-nm output of a pumped dye laser. In the living subjects we determined, for each pulsewidth, the threshold for minimally visible lesions (MVLs). In addition, we noted the energy doses required to induce hemorrhagic lesions relative to the corresponding MVLs and use these data to aid in the interpretation of the damage and energy dispersal mechanisms following absorption of ultrashort laser pulses. The ultrashort-pulse beam was directed through flat preparations of rabbit corneas and vitreous fluid and through intact rabbit lenses. Measurements were made to detect pulsewidth broadening or modulation, spectral broadening or white-light continuum generation, second-harmonic generation, and self-focussing or defocussing. These measurements, chosen as indicators of interactions as the ultrashort pulse passes through the ocular medium, were all negative.

14. SUBJECT TERMS

Cornea; Eye; Femtoseconds; Hemorrhage; Lens; Ocular damage; Picoseconds; Retina; Ultrashort-pulse laser; Vitreous

15. NUMBER OF PAGES

38

16. PRICE CODE

17. SECURITY CLASSIFICATION OF REPORT	18. SECURITY CLASSIFICATION OF THIS PAGE	19. SECURITY CLASSIFICATION OF ABSTRACT	20. LIMITATION OF ABSTRACT
Unclassified	Unclassified	Unclassified	UL

TABLE OF CONTENTS

Page

INTRODUCTION 1

MATERIALS AND METHODS 1

Apparatus 1
In vivo Exposures 2
Isolated Tissue Studies 4

RESULTS 6

In vivo Exposures 6
Isolated Tissue Studies 21

DISCUSSION 24

REFERENCES 28

NOTES ADDED IN PROOF 29

FIGURES

Figure No. — Page

1. Schematic diagram of experimental apparatus 3
2. Dose-response curve and 95% fiducial limits for 4-ns data 7
3. Dose-response curve and 95% fiducial limits for 50-ps data 8
4. Dose-response curve for 5-ps data 9
5. Dose-response curve and 95% fiducial limits for 500-fs data 10
6. Dose-response curve and 95% fiducial limits for 90-fs data 11
7. Fundus photograph at 1-hr postexposure of rabbit retina exposed to 532-nm, 4-ns pulses 14

Figure No. Page

8. Fundus photograph at 24-hr postexposure of rabbit retina seen in Figure 7 14

9. Fluorescein angiogram contact sheet at 1-hr postexposure of rabbit retina seen in Figure 7 17

10. Fluorescein angiogram contact sheet at 24-hr postexposure of rabbit retina seen in Figure 7 19

11. Fluorescein angiogram at 1-hr postexposure of rabbit retina exposed to 580-nm, 5-ps pulses 20

12. Fundus photograph at 1-hr postexposure of rabbit retina exposed to 580-nm, 90-fs pulses 20

13. Fluorescein angiogram contact sheet at 1-hr postexposure of rabbit retina seen in Figure 12 23

14. Fundus photograph of rabbit retina seen in Figure 12 but taken at ~1 hr following exposure to an additional seven suprathreshold pulses 25

15. Experimental ED_{50} retinal damage thresholds plotted on a log-log graph of corneal radiant exposure versus laser pulsewidth 26

TABLES

Table No. Page

1. Laser exposure parameters 6

2. Results of ophthalmoscopic and fluorescein angiography observations 13

3. Comparison of exposure parameters and results from current study with those of Birngruber et al. 27

OCULAR DAMAGE INDUCED BY ULTRASHORT LASER PULSES

INTRODUCTION

The preliminary results presented in this interim report were accomplished under protocol RZV-91-04, "Ocular Effects of Ultrashort-Pulsewidth Laser Radiation."[1] The protocol describes a planned 2-year research effort involving the study of tissue effects of ultrashort laser pulses (nanoseconds (ns) down to $\lesssim$100 femtoseconds (fs)) in the nonhuman primate and rabbit eyes, and in various isolated ocular tissues and tissue models (water, saline, etc.). This report describes that part of the protocol work which was conducted by personnel of KRUG Life Sciences, Incorporated, and Armstrong Laboratory/Optical Radiation Division (AL/OEO) under a 6-month contract extension covering the period from February through July 1992. The remainder of the protocol effort is scheduled to be accomplished under a separate contract with The Analytic Sciences Corporation (TASC).

The details of the work to be accomplished during the contract extension were identified during a series of meetings with the Air Force Contract Monitor (Lieutenant Colonel Robert M. Cartledge) and his technical staff which occurred in February 1992. Through these meetings, the Air Force and KRUG personnel involved agreed that the contract extension effort on this project would be restricted to preliminary threshold estimates of ultrashort-pulse-induced retinal damage in rabbit eyes. In addition, the same rabbit subjects would be used to harvest isolated ocular tissues (to include at least vitreous and lens samples) for studies of laser-beam propagation and damage mechanisms. The laser pulsewidths to be utilized were 4 ns, 50 picoseconds (ps), 5 ps, 500 fs, and $\lesssim$100 fs (the latter being the shortest pulsewidth available from the laser system). Only single-pulse, visible-wavelength exposures were to be covered; the visible wavelength being either doubled neodymium:yttrium-aluminum-garnet (Nd:YAG) or for pulsewidths <50 ps, the ~580-nm wavelength obtained from the dye laser component of the ultrashort-pulse laser system. Ophthalmoscopic and fluorescein angiographic observations were to be carried out at various times postexposure to identify the criteria showing the greatest sensitivity for detecting damage thresholds. These observations were to be supplemented by histopathologic evaluation on selected laser-exposed ocular tissues. The histopathologic evaluation was not part of the in-house effort and will be reported separately.

MATERIALS AND METHODS

Apparatus

The ultrashort-pulse laser system has been described in detail in the experimental protocol for this project[1] and in a technical report detailing the operating procedures for the laser system.[2] The current report describes only the utilization of the ultrashort-pulse system as required to collect the bioeffects data.

The experimental setup for exposing rabbit subjects is straightforward and is depicted in Figure 1. The incident laser beam was apertured to provide a relatively uniform (i.e., square-wave) spatial profile and deliver a beam of $\lesssim$3-mm diameter to the target. The beam diameter at the cornea was limited to this size in order to ensure that the entire beam passed through the pupil regardless of the orientation of the subject's pupil plane, which was adjusted as required to access the various retinal target sites. The aperture was placed so that the laser beam path length from aperture to the target was ~1 m.

The longest pulsewidth studied was ~4 ns. This pulsewidth was achieved by utilizing the Q-switched output of the Quanta Ray GCR-3RA component of the ultrashort-pulse laser system operating in the doubled mode to yield a wavelength of 532 nm. The beam divergence was ~0.5 milliradians (mrad). The laser pulsewidths along with the corresponding wavelengths, beam divergences, and system components utilized to generate each pulsewidth are listed in Table 1.

Single pulses were delivered to the rabbit eye by deflecting the beam off of a pellicle beamsplitter (PB2 in Figure 1) mounted on a Zeiss fundus camera and adjusted such that the deflected beam was colinear with the optical axis of the fundus camera. An attenuated helium-neon laser beam (~0.1 mW) was made colinear to the ultrashort-pulse laser beam and was used in aligning the subject and to designate the selected retinal exposure sites as viewed through the fundus camera. The subject was mounted on an adjustable stage with the corneal plane ~1 cm in front of the pellicle beamsplitter.

To measure the energy delivered by each pulse, a Molectron JD2000 joulemeter/ ratiometer was used with a J309 or J409 detector head placed at the eye position and calibrated against a second head mounted to intercept the fraction of the beam deflected by the first pellicle beamsplitter (PB1 in Figure 1). Cross-calibration between the two detector heads was accomplished at the onset of each exposure session and was rechecked just after exposures were completed. Calibration uncertainty for the detector heads is quoted by the manufacturer as ±7%.

Laser pulse energy was controlled by rotation of a half-wave plate inserted before the amplifier stages of the ultrashort-pulse system. (Only the vertical polarization component was amplified.) However, shot-to-shot variability in pulse energy proved to be a problem especially when selecting energies near the bottom of the range available by rotating the half-wave plate. In those cases, variability was sometimes ±50% or more of the average pulse output.

In vivo Exposures

The experimental subjects were mature Dutch-Belted rabbits ranging in size from 1.5 to 2.5 kg. Prior to being assigned to the experimental protocol, subjects received an initial ophthalmic screening to ensure clear ocular media, normal fundi, and refractive error differences of no more than 0.5 diopter in any meridian. Quantitative records of the refractive measurements were not maintained.

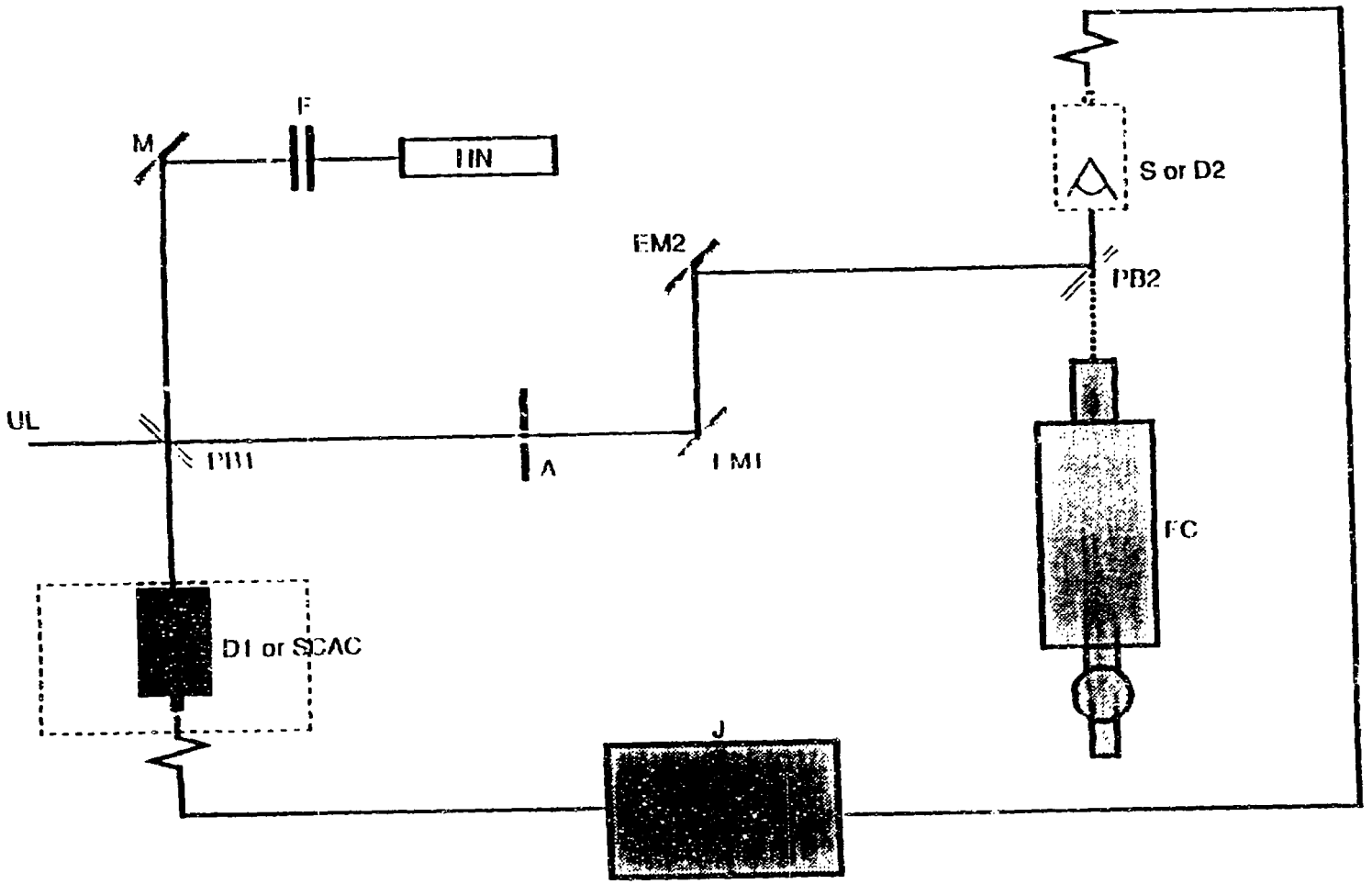

Figure 1. Schematic diagram of experimental apparatus.

UL - Ultrashort-pulse laser beam
PB1,2 - Pellicle beamsplitters
M - Mirror
EM1,2 - Beam-elevating mirrors
D1,2 - Detector heads
SCAC - Slow-scan autocorrelator

J - Joulemeter
A - Aperture
F - Neutral-density filter(s)
HN - HeNe alignment laser
FC - Fundus camera
S - Subject

Approximately 24 hr prior to exposures, topical ophthalmic atropine sulfate (1%) was administered into each subject's conjunctival sac to induce cycloplegia. The animals were anesthetized with an intramuscular injection of ketamine (30 mg/kg body weight) and xylazine (18 mg/kg body weight). Oculostasis was maintained throughout the exposure session by intravenous injection, to effect, of a mixture of ketamine/xylazine (3:1.8; diluted in lactated Ringer's to a combined concentration of 50 mg/ml) into the marginal ear vein. The cornea was irrigated frequently with lactated Ringer's to prevent desiccation. Preexposure screenings and postexposure examinations were carried out with a Zeiss fundus camera. When fluorescein angiography was required, 10-15 mg/kg body weight fluorescein was injected into the ear vein.

The anesthetized subject was first placed in a restraint box which was mounted on the adjustable stage in front of the fundus camera. The subject was positioned so that the retina of the chosen eye was brought into the focal plane of the fundus camera and was viewed through the pellicle beamsplitter (PB2). Exposures were delivered to sites arranged in a rectangular grid pattern located below the visual streak. For some exposure regimes (the longer pulsewidths), threshold lesion development was nearly immediate, and alternate supra- and subthreshold exposure doses resulted in a systematic definition of the exposure grid as the exposure session progressed. For shorter pulsewidths ($\lesssim$5 ps), threshold lesion development took some time (up to tens of minutes) so the exposure session began with a series of high-dose exposures which quickly developed to 100-200-μm diameter marker lesions. The lower experimental doses were then delivered to the grid sites predefined by the marker lesions.

Following completion of the laser exposures, the subject was transferred to a second fundus camera station which allowed direct viewing of the retina (without a beamsplitter placed in front of the subject's eye) and which was set up for routine 35-mm photography as well as for the filtered, timed photography conducted for the fluorescein angiography assessment of retinal damage.

Isolated Tissue Studies

The rabbit subjects were also used as the source for ocular tissues (cornea, lens, and vitreous) used to investigate the propagation effects of ultrashort laser pulses in the ocular medium. In those cases, the subjects were first anesthetized with a mixture of ketamine (30 mg/kg body weight) and xylazine (18 mg/kg body weight) injected intramuscularly. An intravenous catheter was placed in the marginal ear vein. Eyelids were retracted with a pediatric speculum. Just prior to enucleation, a lethal dose (~120 mg/kg body weight) of sodium pentobarbital was administered intravenously.

The conjunctiva was parted with scissors around the orbit. The eye muscles were retracted with an eye muscle hook and severed with scissors; then, the eyeball was lifted with forceps and the optic nerve severed with enucleation scissors. The eyeball was removed from the socket and placed on sterile gauze pads moistened with balanced salt solution (B.S.S.).

A circular incision was made around the central cornea with a corneal trephine. The incision was completed with curved iris scissors and a disc of central cornea removed, using caution not to mar the surface, and placed between two quartz plates. The tissue was bathed in B.S.S. to prevent desiccation. The quartz plates had lips such that fitting the two quartz pieces together formed a quartz cuvette which then maintained the cornea and B.S.S. contents while the laser-pulse propagation studies were completed.

An incision was made in the orbit just posterior to the *ora serrata* using a #11 surgical blade and continued around the orbit with curved iris scissors until the anterior chamber was free from the posterior capsule. The anterior chamber was removed and placed inverted on moist sterile gauze pads. Vitreous was harvested from the posterior capsule with forceps and scissors and placed in a quartz cuvette.

The lens was removed by carefully severing the suspensory ligaments of the ciliary body, lifted with a lens loop, and placed into a quartz cuvette where it was kept moist with B.S.S.

Once the ocular tissue sample (cornea, lens, or vitreous) was secured in the quartz cuvette, the following measurements were conducted on propagation of ultrashort laser pulses through the cell:

1. Absorption measurements - The joulemeter/ratiometer was used to measure the loss of pulse energy in passing through the cell. Full-scale deviation from linearity for the Molectron meter was 1%.

2. Pulsewidth broadening or modulation - The slow-scan autocorrelation measurements used to characterize the pulsewidth[1,2] were repeated on laser pulses which had passed through the cell. Temporal resolution of the slow-scan autocorrelator was 20 fs.

3. Spectral broadening or white-light continuum generation - The scanning monochromator measurements used to characterize the fundamental wavelength and bandwidth[1,2] were repeated on pulses which had passed through the cell. The monochromator bandwidth was <1 nm for the 150-μm slits which were utilized whereas the bandwidth of the pulses emitted from the dye laser was ~6 nm.

4. Second-harmonic generation - The scanning monochromator was also used to determine if passing through the cell resulted in second-harmonic generation. Absolute sensitivity was ~1 μJ and since >100 μJ per pulse was available for all pulsewidths, a doubling efficiency as low as 1% would be detectable.

5. Beam divergence - Visual observations were made of spot size at several distances beyond the sample cell to determine if the nominal beam divergence (Table 1) changed after passing through the cell.

Table 1. Laser Exposure Parameters.

Pulsewidth (ps)	Wavelength (nm)	Divergence (mrad)	Laser Source
4000	532	0.5	Q-switched Nd:YAG
50	532	0.5	Regenerative amplifier--Nd:YAG
5	576	≤1.0	Amplified pulsed dye laser
0.5	580	~2.0	Amplified pulsed dye laser
0.09	580	≤1.0	Chirped and amplified pulsed dye laser

All of these measurements were conducted on empty cells, saline cells (cuvettes filled with B.S.S.), and sample cells containing either vitreous fluid or corneal or lens samples immersed in B.S.S. The measurements were conducted for several laser pulsewidths and peak-power levels representative of those used for the *in vivo* exposures.

RESULTS

In vivo Exposures

For each of the pulsewidths listed in Table 1, preliminary retinal damage threshold data was collected using two to four rabbit eyes. On average, ~20 experimental exposures were delivered to each eye. Following each exposure, the immediate ophthalmoscopic observations were recorded, and lesion or hemorrhage development was periodically monitored until 1-hr postexposure. At 1-hr postexposure, ophthalmoscopic lesion/no-lesion data were recorded, and probit calculations were carried out based on the 1-hr data. Fluorescein injection was performed immediately after the 1-hr ophthalmoscopic readings and lesion/no-lesion notations taken based on the fluorescein visualization of the fundus. With most subjects, both the ophthalmoscopic and the fluorescein readings were repeated at ~24-hr postexposure. On a few subjects the readings were also repeated at later times (48 hr or 72 hr), but further follow-up readings were discontinued, as no notable changes in development of retinal lesions were apparent beyond 24 hr.

Figures 2 through 6 show plots of the 1-hr postexposure ophthalmoscopic lesion/no-lesion data together with the dose-response curves and 95% confidence intervals calculated by

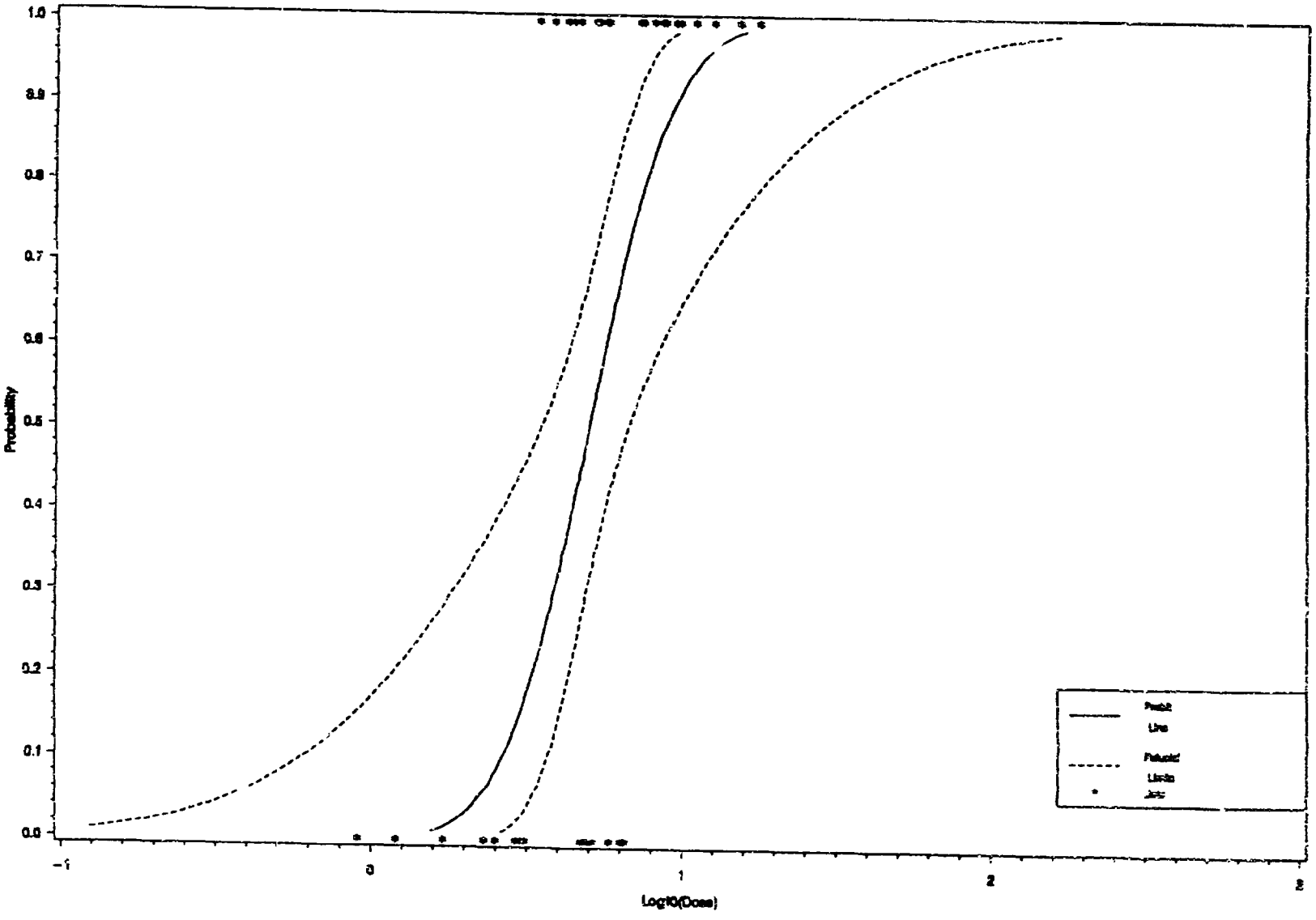

Figure 2. Dose-response curve and 95% fiducial limits for 4-ns data (*).

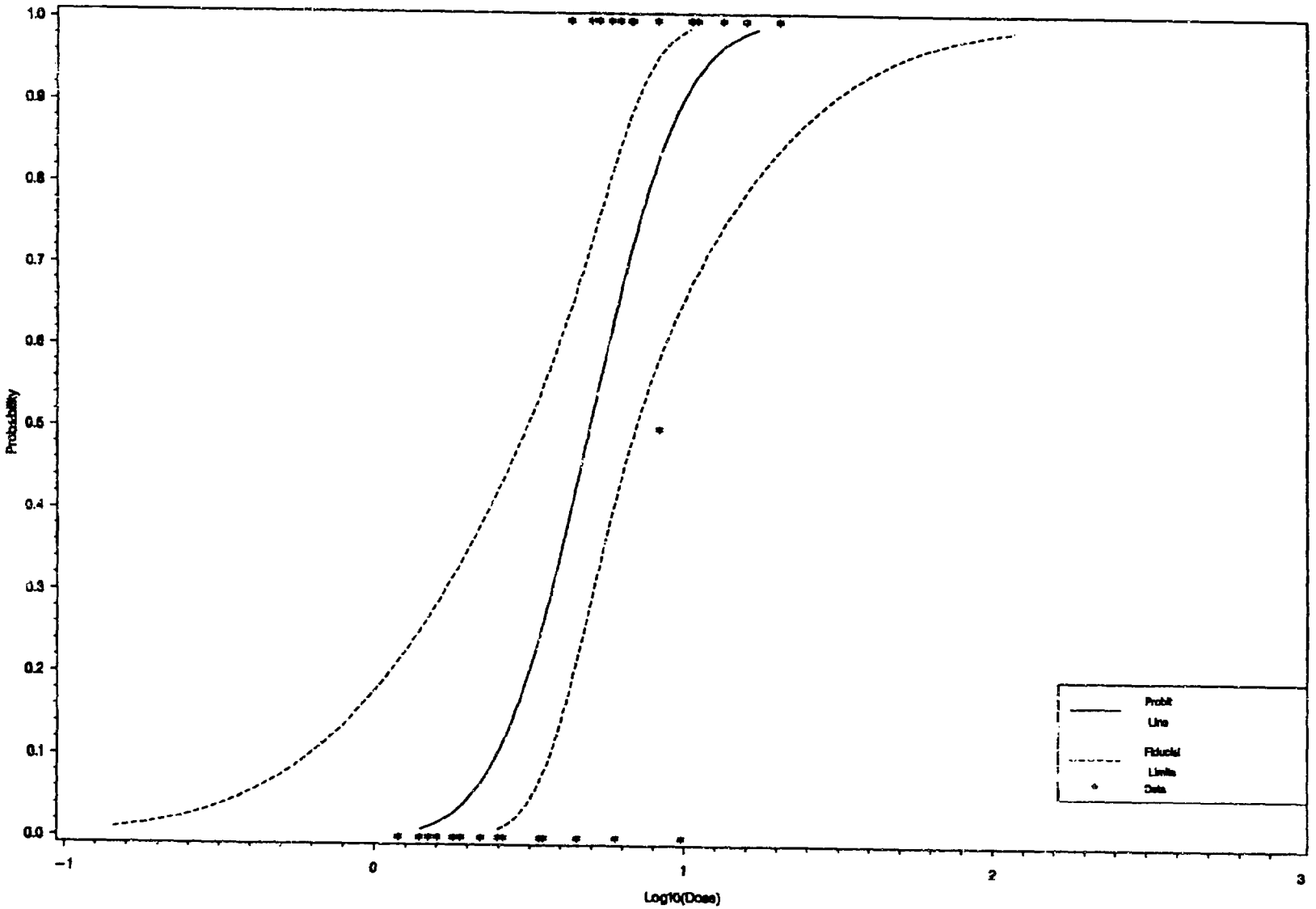

Figure 3. Dose-response curve and 95% fiducial limits for 50-ps data (*).

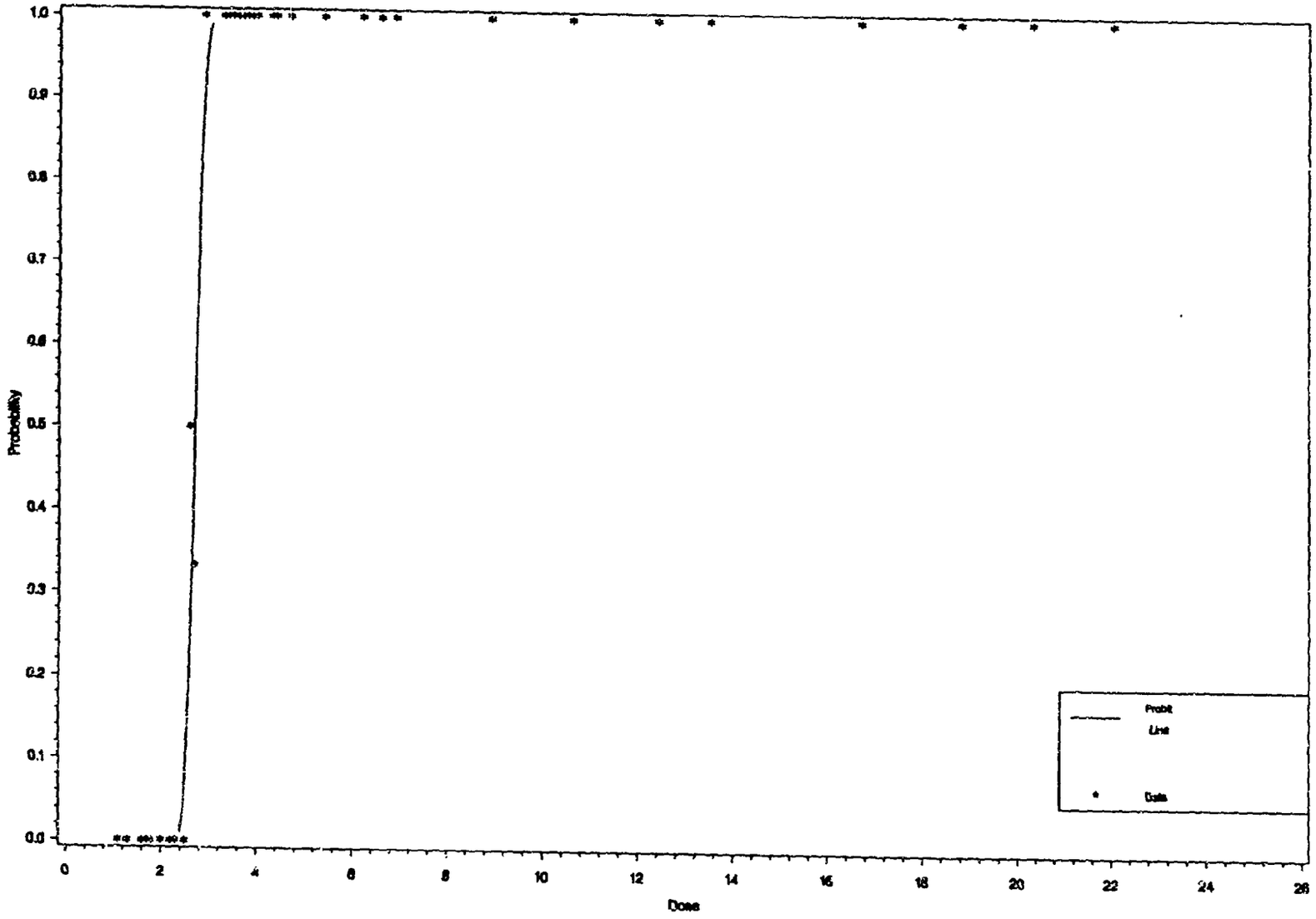

Figure 4. Dose-response curve for 5-ps data (*).

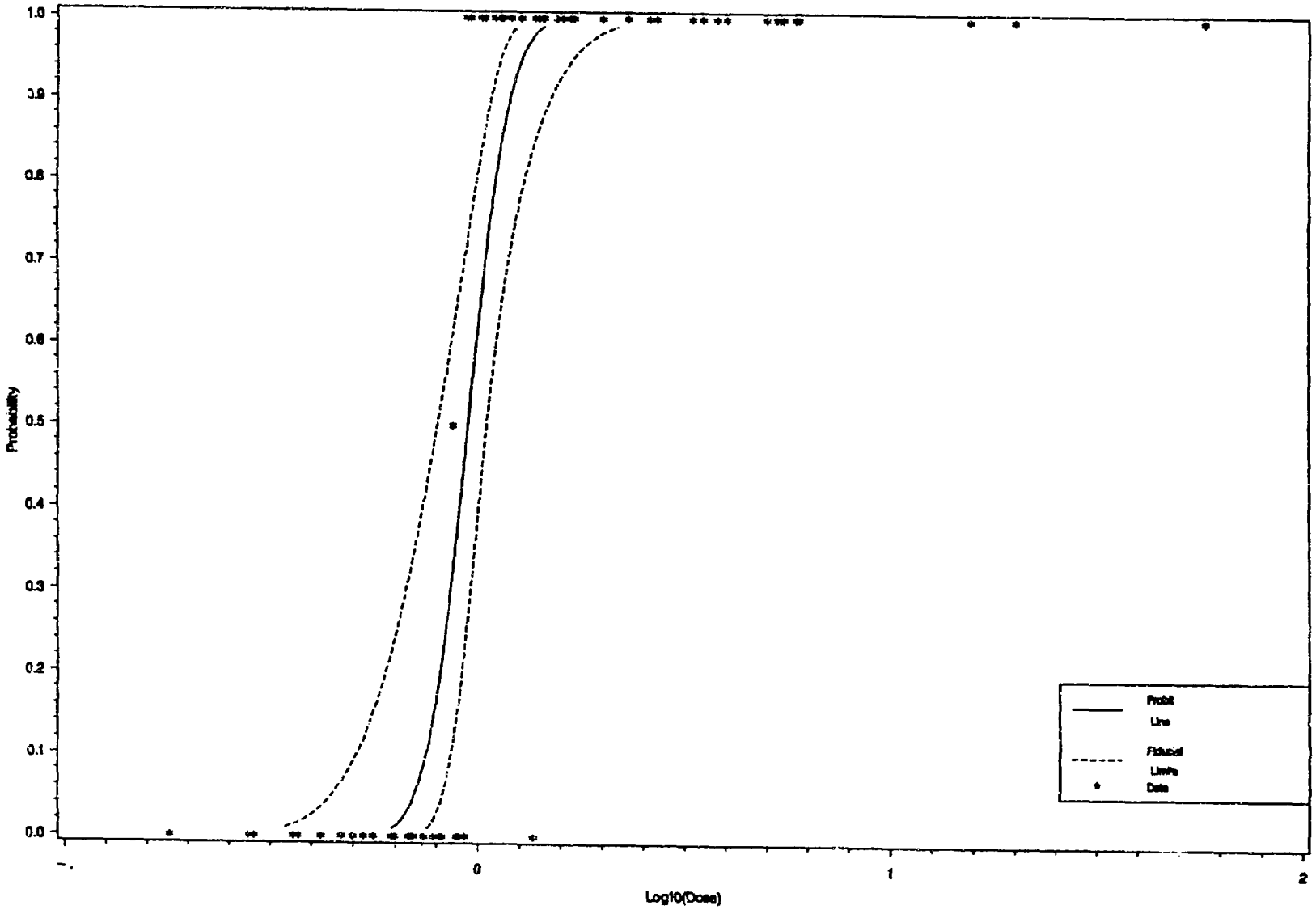

Figure 5. Dose-response curve and 95% fiducial limits for 500-fs data (*).

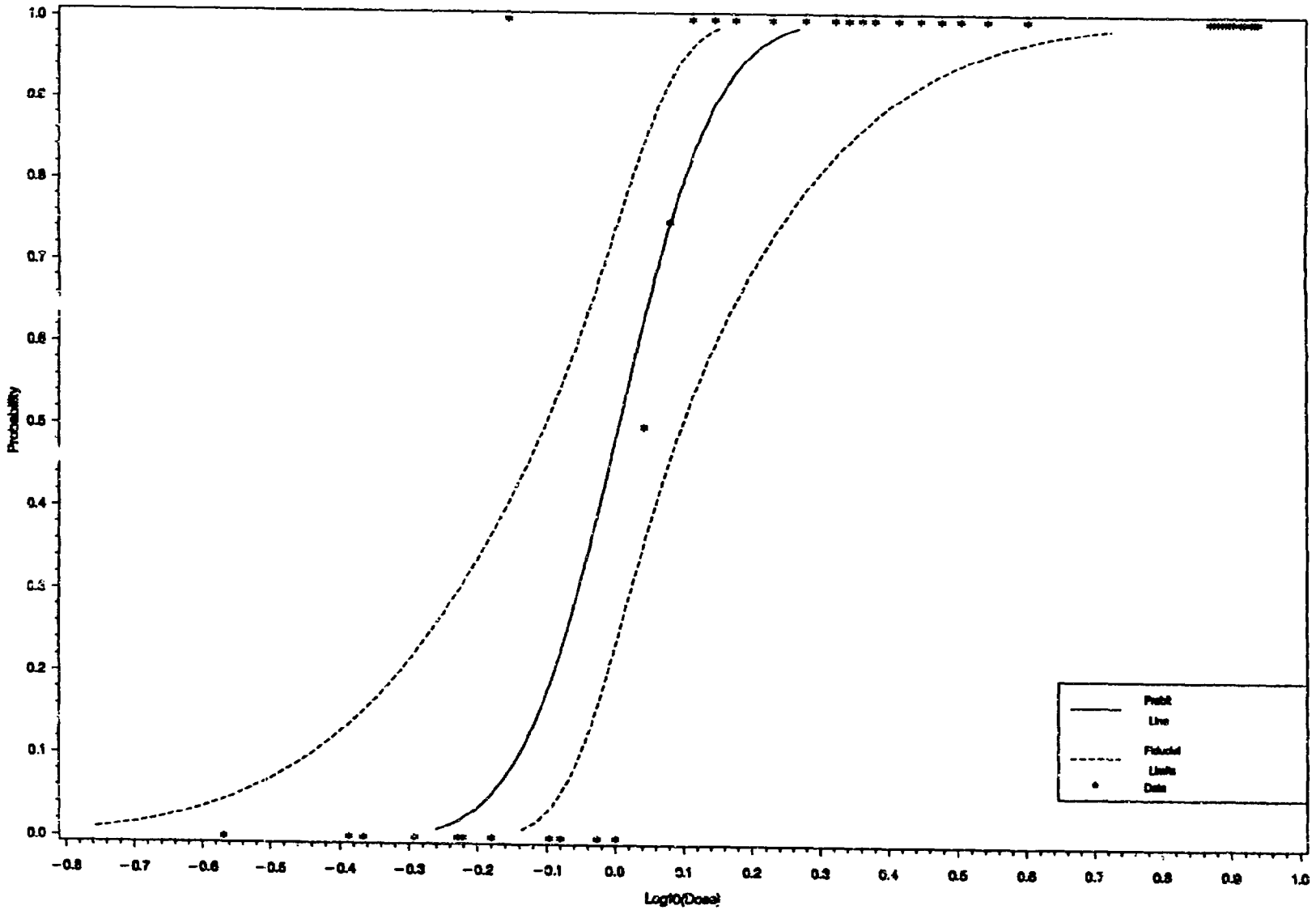

Figure 6. Dose-response curve and 95% fiducial limits for 90-fs data (*).

probit analysis*. The plots for the five pulsewidths appear in the order listed in Table 1. Data points are plotted at the experimental frequency of lesion observation (i.e., "no-lesion" data are plotted at 0% probability, "lesion" data at 100% probability and, for example, if three exposures at dose "x" resulted in one lesion and two no lesions, the plot shows one point with coordinates (x, 0.33)). The graph for 5-ps pulsewidths (Figure 4) has no confidence limits since they were not generated by the probit calculation. In this case, there was only a very narrow band of overlap between the dose range which yielded lesions and that which yielded no lesions. The probit program could not define a slope (with high confidence) for this narrow overlap region, or more specifically, could not distinguish the slope from infinity. Hence, the 95% confidence interval was not defined--but see notes added in proof.

The median effective dose (ED_{50}) threshold values and confidence intervals calculated on the basis of the 1-hr ophthalmoscopic readings are summarized in Table 2. It must be reiterated that these are preliminary threshold estimates based on data from only two to four eyes per estimate. The problem with basing the estimates on so few eyes is that the subject-to-subject variability in sensitivity to laser-induced retinal damage can be (and sometimes is) great enough to undermine the seemingly well-behaved probit calculations.

Several additional columns of data are included in Table 2. With the longest pulsewidth utilized (4 ns), threshold retinal lesions were generally visible almost immediately after exposure and showed little further development with time postexposure. Also, the majority of suprathreshold exposures resulted in hemorrhagic lesions. Typical results for 4-ns exposures are seen in Figures 7 through 10. Figure 7 is a fundus photograph taken at ~1 hr following a sequence of 12 exposures ranging in dose from 4.7 μJ to 9.7 μJ (all energy readings are subject to the ±7% calibration uncertainty of the detectors). It is seen that six of the exposures resulted in hemorrhagic lesions, all of which were immediately apparent. Three additional exposures yielded small lesions without hemorrhaging. These lesions were not noted immediately following exposure but were discernible within several minutes postexposure. Figure 8 shows the same fundus at 24-hr postexposure. There is no further development of small nonhemorrhagic lesions, but the hemorrhages are distinctly larger in size although in some cases the blood has already begun to resolve from the center of the lesions. Figures 9 and 10 show the results of fluorescein angiography on the same eye at 1-hr and 24-hr postexposure, respectively. The first two frames (on the bottom line of each photo) were taken before the fluorescein was injected and are merely red-light-free equivalents of the photographs reproduced in Figures 7 and 8. The remaining frames show the time evolution of the fluorescein leakage (moving from right to left and bottom to top) in the several minutes following injection. The hemorrhagic lesions appear as dark spots since the blood blocks the view of any fluorescein leakage in the underlying or coincident tissue layers. The nonhemorrhagic lesions noted on the fundus photos (Figures 7 and 8) are also apparent by fluorescein angiography, but the fluorescein did not result in visualization of any additional lesions at either 1-hr or 24-hr postexposure.

*SAS package of statistical programs, Version 6, SAS Institute Inc., 1989

Table 2. Results of Ophthalmoscopic and Fluorescein Angiography Observations.

Pulsewidth (ps)	MVL Threshold[1] (1-hr, μJ)	Rapid Lesion Development?	Further Lesion Development by 24-hr Postexposure?	Fluorescein Threshold less than MVL Threshold?		Hemorrhage Threshold (μJ)
				1-hr	24-hr	
4000	5.0 (3.5-6.6)	Yes	No	Marginal	No	~7 (most)[4]
50	4.9 (3.1-6.9)	Yes	No	Marginal	No	~10 (most)
5	2.7[2]	No[3]	Marginal	Marginal	No	>10 (few)
0.5	0.94 (0.80-1.0)	No[3]	No	Significant (≤0.4 μJ)	No (greater)	>10 (few)
0.09	1.0 (0.79-1.2)	No[3]	No	Marginal	No	>100 (none)

[1]95% confidence intervals except where noted.
[2]95% confidence interval could not be calculated from original data. See notes added in proof.
[3]Takes tens of minutes to develop to ultimate lesion size.
[4]Most exposures at this dose yield hemorrhagic lesions.

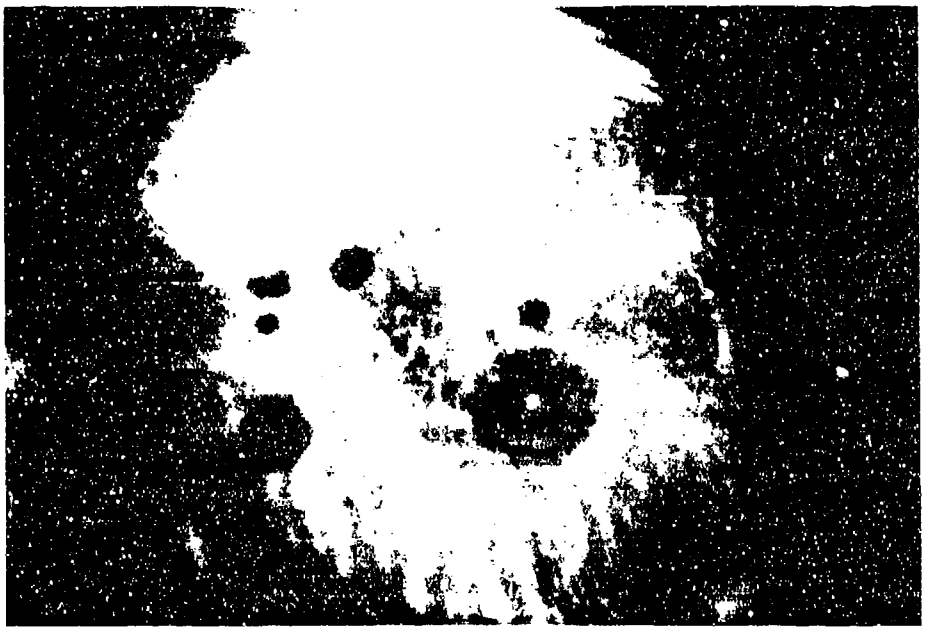

Figure 7. Fundus photograph at 1-hr postexposure of rabbit retina exposed to 532-nm, 4-ns pulses.

Figure 8. Fundus photograph at 24-hr postexposure of rabbit retina seen in Figure 7.

For shorter pulsewidths, the threshold lesions developed more slowly and, for ≤5-ps pulses, took from several minutes to one hour to reach their ultimate size. In every case, however, the lesion development had stabilized by ~1-hr postexposure, and in only one case (5-ps pulses) was the 24-hr ophthalmoscopic threshold even marginally lower than at 1 hr. Fluorescein readings at 1-hr postexposure generally resulted in visualization of all lesions that were ophthalmoscopically visible plus isolated instances of visualization of lesions resulting from slightly lower exposure doses. Figure 11 shows an enlargement of one frame from the fluorescein angiography performed at 1-hr postexposure on an eye which received a total of 22, 5-ps exposures ranging in energy from 1.7 μJ to 22 μJ. The higher exposure doses associated with the bottom two rows of lesions yielded immediately visible bright spots, but the remaining exposures (≤5 μJ) yielded no immediate lesions, although all 22 lesions were visualized with the 1-hr fluorescein angiography. As seen from Figure 11, two hemorrhages were apparent (from doses of 6.6 and 6.9 μJ). Less obvious from this photograph is a third hemorrhage (from a dose of 16.7 μJ) which was ophthalmoscopically visualized as a small red spot superimposed on a bright white lesion. After learning from the first eye exposed to 5-ps pulses that lesion development time was slower than for the longer-pulse cases, subsequent experiments with 5-ps and shorter pulsewidths proceeded by first delivering a sequence of high-power exposures to create a row and column of marker lesions and then delivering the lower power doses to the grid sites defined by the markers.

For 500-fs pulses only, the 1-hr fluorescein threshold was significantly lower than the 1-hr ophthalmoscopic threshold (Table 2). In contrast, with 500-fs pulses, fluorescein visualization at 24-hr postexposure implied a higher threshold than found at 1 hr by either ophthalmoscopic or fluorescein observation. However, in general, at 24-hr postexposure, lesion appearance (both ophthalmoscopic and fluorescein visualization) was similar to that at 1 hr. Also, by 24-hr postexposure, the "redness" associated with fresh hemorrhagic lesions had sometimes faded, but there was no change in ophthalmoscopic or fluorescein lesion/no-lesion readings which would have affected the threshold doses.

The final sequence of photographs depicts an eye exposed to the shortest pulsewidth available for this study (~90 fs). Thirty exposures were delivered to the eye shown in Figures 12 and 13. The first 10 exposures were all at a dose of ~8 μJ (range: 8.0 to 8.7 μJ) and served to provide marker lesions ~150 ±50 μm in diameter. These exposures are readily apparent both ophthalmoscopically (Figure 12) and with fluorescein (Figure 13). The remaining exposures spanned a range of 0.43 to 4.0 μJ, bracketing the ED_{50} threshold dose of 1.0 μJ. None of these exposures yielded effects which were ophthalmoscopically visible within a few minutes postexposure. By 1-hr postexposure, small lesions estimated at 30-50-μm diameter were discernible by both ophthalmoscopic and fluorescein visualization.

During a subsequent experimental session, the same eye was exposed to suprathreshold doses ranging from ~8 μJ to 120 μJ. The resulting lesions, seen in Figure 14, ranged up to ~500 μm in diameter but had a more diffuse appearance than the smaller, brighter marker lesions seen in Figure 12. No hemorrhages were found, which agrees with the report of Birngruber et al.[5] Although we did not quantitatively study lesion size as a function of pulse

Figure 9. Fluorescein angiogram contact sheet at 1-hr postexposure of rabbit retina seen in Figure 7. Red-free fundus photographs on bottom row were taken before fluorescein was injected.

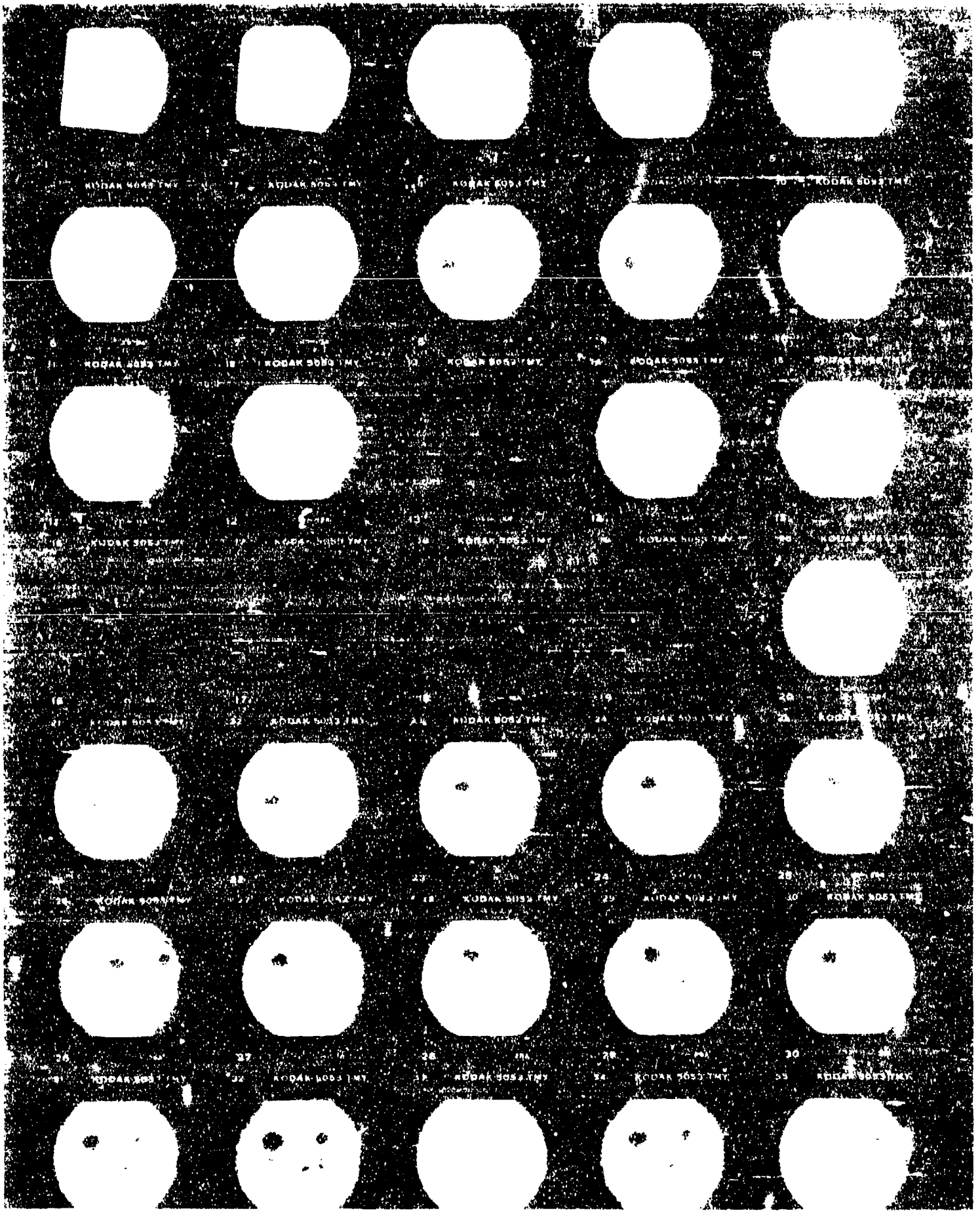

Figure 10. Fluorescein angiogram contact sheet at 24-hr postexposure of rabbit retina seen in Figure 7. Red-free fundus photographs on bottom row were taken before fluorescein was injected.

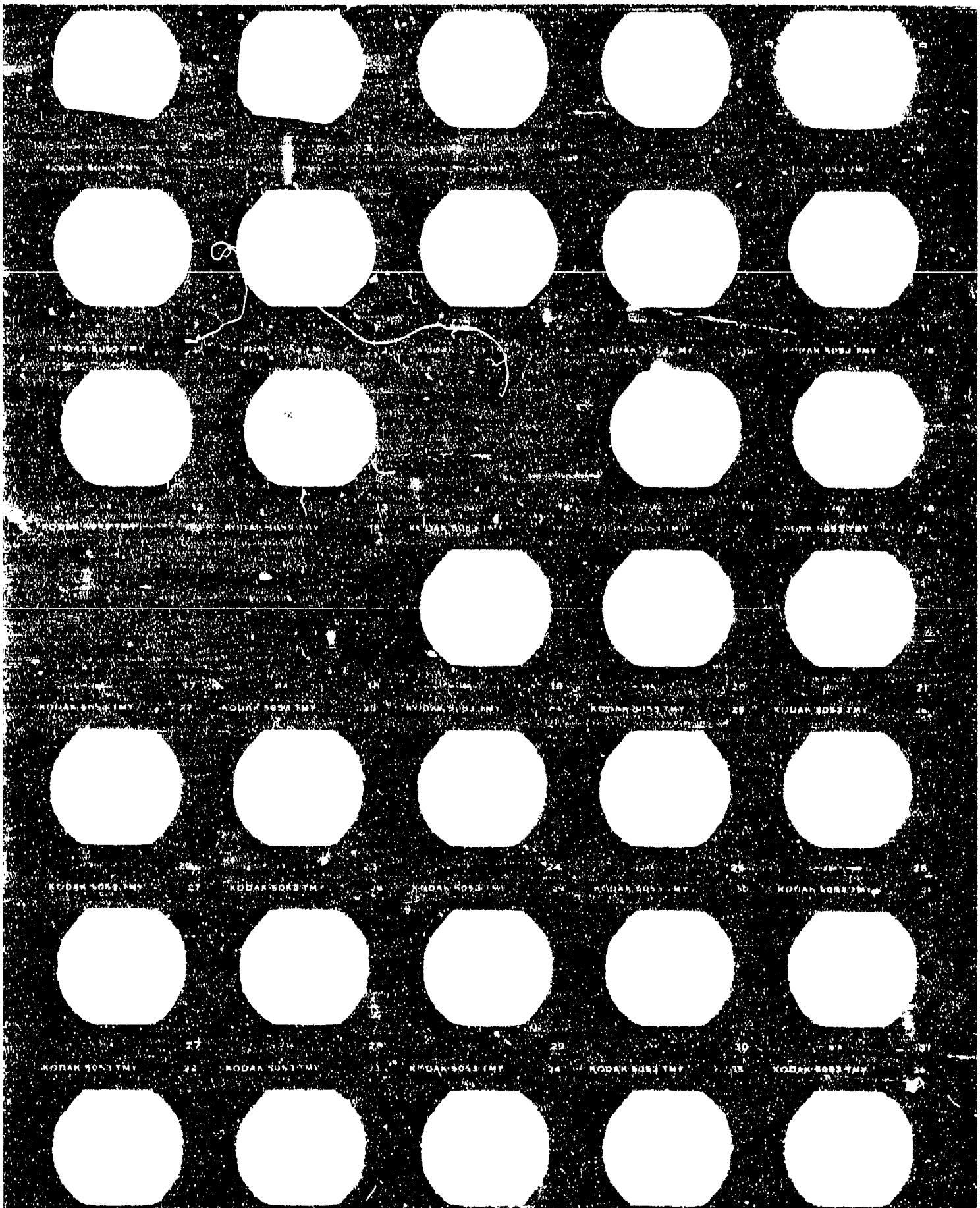

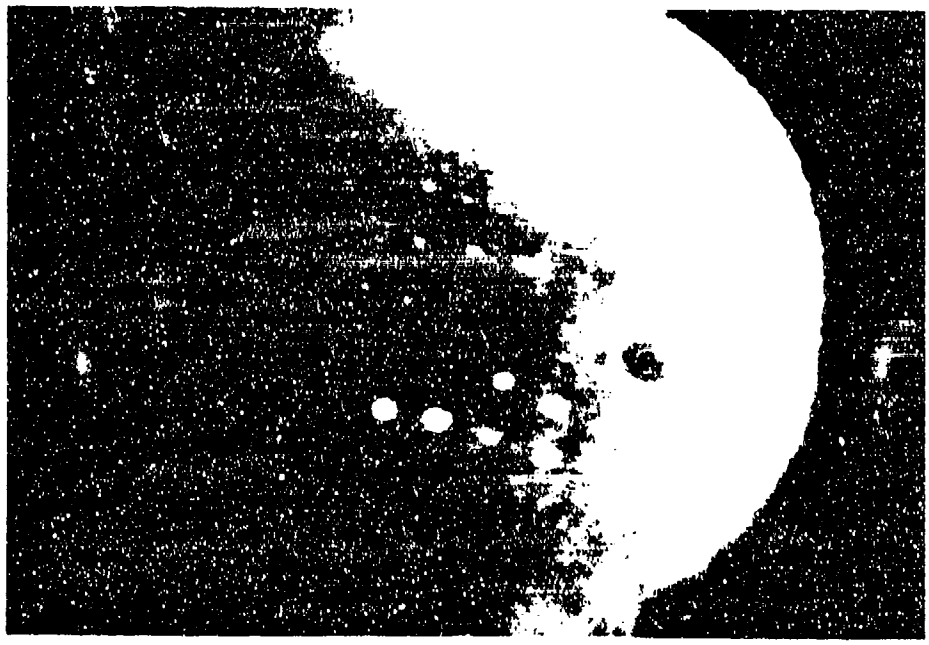

Figure 11. Fluorescein angiogram at 1-hr postexposure of rabbit retina exposed to 580 nm, 5-ps pulses.

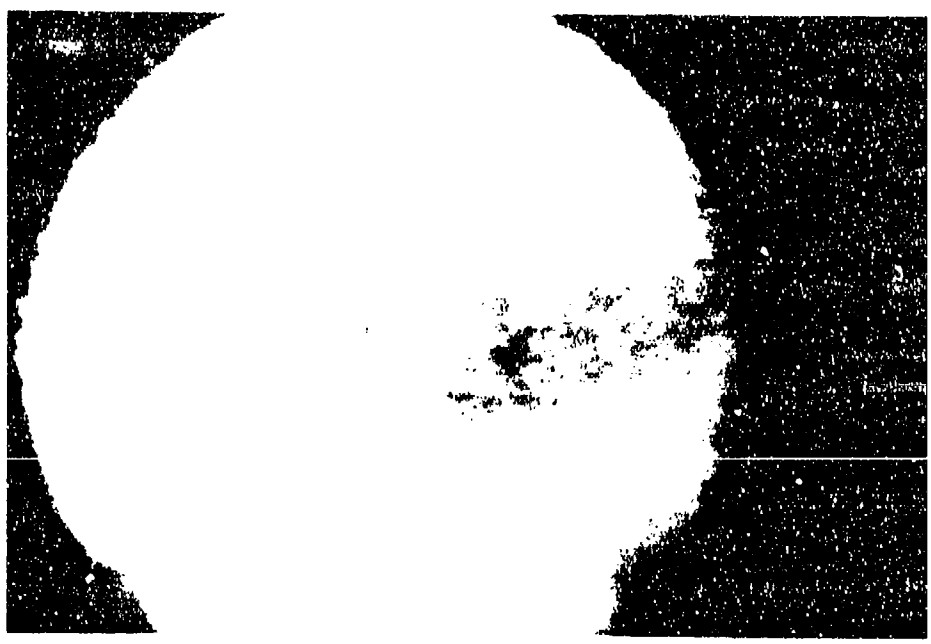

Figure 12. Fundus photograph at 1-hr postexposure of rabbit retina exposed to 580-nm, 90-fs pulses.

energy, the trend noted here is consistent with that reported in retinal damage studies utilizing longer pulsewidths.[6]

No attempt was made to collect additional data for quantitating hemorrhage thresholds. The following incidental observations are reported based on our findings while collecting data to estimate minimal visible lesion (MVL) thresholds:

The minimal hemorrhage threshold for 4-ns pulses was only marginally higher than the corresponding MVL threshold (i.e., almost every exposure which resulted in a "lesion" for purposes of calculating the MVL threshold also produced at least a minimal hemorrhage). As the pulsewidth decreased, the MVL threshold trended lower (see Table 2), but the hemorrhage threshold appeared to increase. Nevertheless, except for the 90-fs pulses, the exposure doses utilized to collect MVL threshold data occasionally resulted in hemorrhagic lesions. With 90-fs pulses, no hemorrhages were found, even the maximum pulse energy available (~120 μJ) which was ~120 times the MVL threshold.

Isolated Tissue Studies

None of the preliminary experiments designed to detect laser-tissue interactions as the ultrashort laser pulses propagated through isolated ocular tissues yielded a positive result. That is, using pulse energies comparable to or greater than those used for the *in vivo* exposures, absorption of the basically transparent samples was negligible, and no changes in the temporal profile, spectral content, or beam divergence were observed when the pulses passed through the cornea, lens, vitreous, or saline-filled cuvettes. For the temporal profile this means that, to within the 20-fs resolution of the slow-scan autocorrelator, the pulsewidth and the overall temporal profile were unchanged in passing through any sample cell. Using the scanning monochromator, to within the 1-nm bandwidth of the instrument, no broadening or structure was seen on the inherent laser emission bandwidth. Further, no emission was found at the doubled wavelength of the fundamental laser pulse. The beam divergence (as estimated by visualizing the pulse off of a reflecting surface placed at various distances beyond the sample cells) was also unchanged except for the lens samples, where the divergence matched that expected for a focussing lens of equivalent power. The corneal samples, being flat preparations, as well as the vitreous and saline cells did not perceptibly change the beam divergence.

In addition to these experiments, we utilized 1064-nm, 50-ps pulses, where energies of up to 100 mJ/pulse were available. A search was conducted for indications of laser-tissue interactions when the 1064-nm pulses were directed through an excised rabbit cornea. Again all results were negative until the maximum available peak power at the cornea was utilized (~10^{10} W/cm^2). At this power level, a trace of green light was generated when the laser pulse passed through the isolated cornea, whereas none was seen when an empty cell was used as the target. This presumed wavelength doubling was too weak to allow quantitative determination of the doubling efficiency. Given the 1-μJ sensitivity of the detector, the doubling efficiency for 100-mJ incoming pulses was $\lesssim 10^{-5}$. Hochheimer reported a doubling efficiency of 6 x 10^{-9}

Figure 13. Fluorescein angiogram contact sheet at 1-hr postexposure of rabbit retina seen in Figure 12.

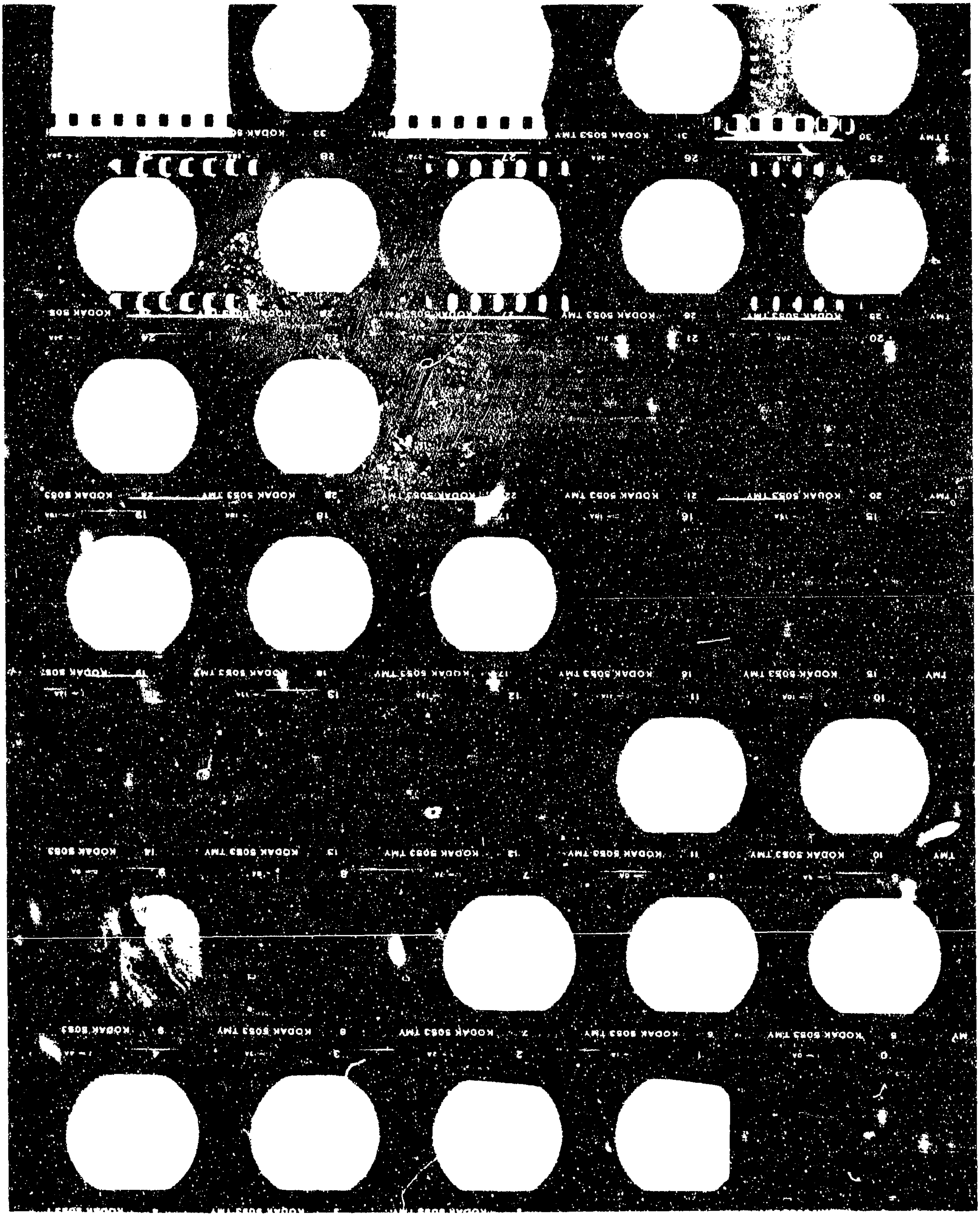

for 1064-nm laser pulses passing through the rabbit cornea with an input power density of 10^6 W/cm^2.[7] Theoretically, assuming that the doubling efficiency increases as the square of the power density, the efficiency would be pushing the limit of unity with the 10^{10} W/cm^2 available here and should be high enough to be quantitatively measured with the current apparatus whenever the input power density exceeded ~10^8 W/cm^2. Apparently, under the conditions of this experiment, the doubling efficiency does not track with the square of the power density for densities $\geq 10^8$ W/cm^2. In any event, since the density of ~10^{10} W/cm^2 exceeded the corneal power densities by orders of magnitude for all *in vivo* exposures in this study, it seems unlikely that wavelength doubling in the anterior ocular tissues plays any role in the retinal damage induced by ultrashort laser pulses.

DISCUSSION

As seen from Table 2, there is a decreasing trend of ophthalmoscopic lesion threshold with decreasing pulsewidth. However, these data imply a relatively shallow slope to that trend as the threshold decreases by less than one order of magnitude as the pulsewidth varies by nearly five orders of magnitude (4 ns to 90 fs). Figure 15 shows the preliminary thresholds from the current study added to the standard plot of MVL threshold versus pulsewidth. The figure also demonstrates the relationship between the maximum permissible exposure (MPE) laser safety standards[3,4] and the experimental threshold data. The data from our study imply little deviation with decreasing pulsewidth from the horizontal MPE lines which apply to pulsewidths from 1 ns to 18 μs. At most, there is a slight decreasing trend in threshold (and, therefore, in MPE) with decreasing pulsewidth as suggested by the dashed line drawn on Figure 15. A linear regression fit of MVL threshold as a function of pulsewidth for the four sub-ns data points listed in Table 2 yields a line with a slope of 0.072 μJ/ps (correlation coefficient = 0.94). When the 4-ns datum is included in the fit, the slope decreases to 0.0067 μJ/ps (correlation coefficient = 0.59). The later fit is presumed to be less reliable since there is no evidence that the MVL threshold, after being nominally flat from 18 μs to 1 ns, begins to trend downward at ~1 ns. In fact, since the 50-ps threshold is not significantly lower than the 4-ns threshold, the downward trend may only be applicable to pulsewidths $\leq$50 ps. Additional threshold data in the fs-ns range are required to support this suggestion.

The information compiled in Table 2 may indicate a change in damage mechanism or laser-tissue interaction as the pulsewidth is decreased below ~50 ps. The MVL threshold for 5 ps and shorter pulses is less than that observed with 50 ps and longer pulses--although as just noted, the decrease is not dramatic. For 50 ps and longer pulses, threshold lesions generally become apparent almost immediately following exposure and show little further development in size or contrast after the first few minutes postexposure. Suprathreshold exposures result in immediate lesions which may take some minutes (but less than 1 hr) to develop to their ultimate size. In contrast, with 5 ps and shorter pulses, we found that threshold doses and even the suprathreshold doses used to produce marker lesions (i.e., up to about an order of magnitude above threshold) yielded no immediately visible retinal disruption. Rather the lesions developed more slowly over a period of up to 1 hr following exposure. The ultimate lesion size was roughly proportional to dose.

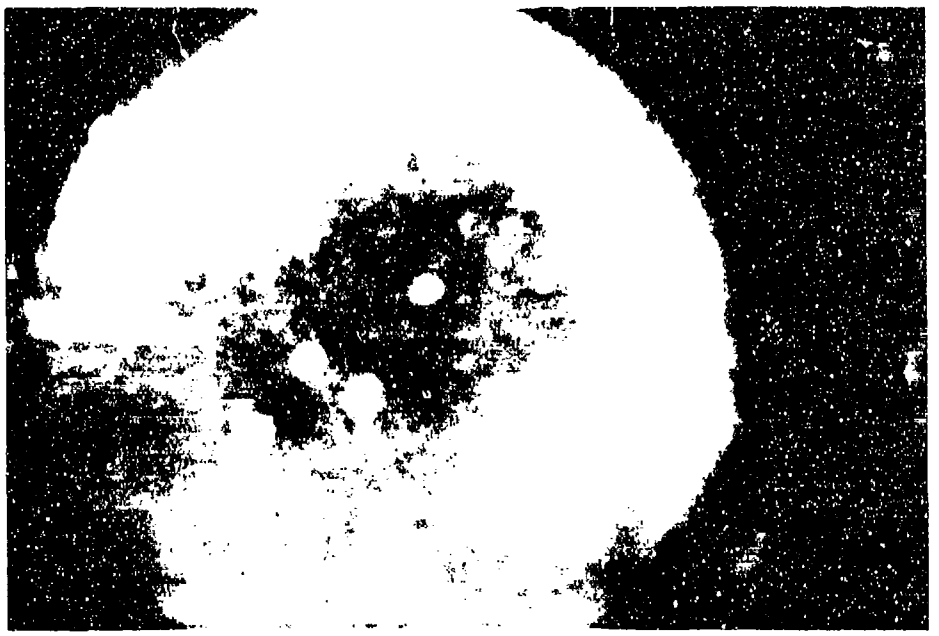

Figure 14. Fundus photograph of rabbit retina seen in Figure 12 but taken at ~1 hr following exposure to an additional seven suprathreshold pulses. The added exposures were also 580-nm, 90-fs pulses with energy doses ranging from 8 μJ to 120 μJ.

The 5-50-ps pulsewidth range also seems to encompass a change in the efficiency of hemorrhage production. For 50-ps and 4-ns pulses where the MVL threshold is ~5 μJ incident at the cornea, the majority of suprathreshold exposures resulted in hemorrhagic lesions. For 5-ps and 500-fs pulses, the same 5-10-μJ exposure dose range (which in these cases was used to produce marker lesions) resulted in only a small percentage of hemorrhagic lesions. With 90-fs pulses, no hemorrhages could be produced even with exposure doses up to 120 μJ. (See notes added in proof.)

Our results for 90-fs, 580-nm pulses can be compared to those of Birngruber et al.[5] who utilized 80-fs, 625-nm pulses (see Table 3). One difference in experimental approach was that Birngruber et al.[5] used a controlled 50-μm retinal spot size, whereas our study allowed the collimated laser beam to be focused by the eye. The optical quality of the rabbit eye is poor relative to that of the primate, and the minimum retinal spot size has been estimated by various sources to be between 50 and 100 μm in diameter. The approach of Birngruber et al.[5] required that a Goldman (plano-concave) contact lens be placed on the rabbit cornea to negate its optical power. In our study, no corrective lenses were used in order to avoid the potential complication of the ultrashort laser pulses interacting with the lens material. These factors

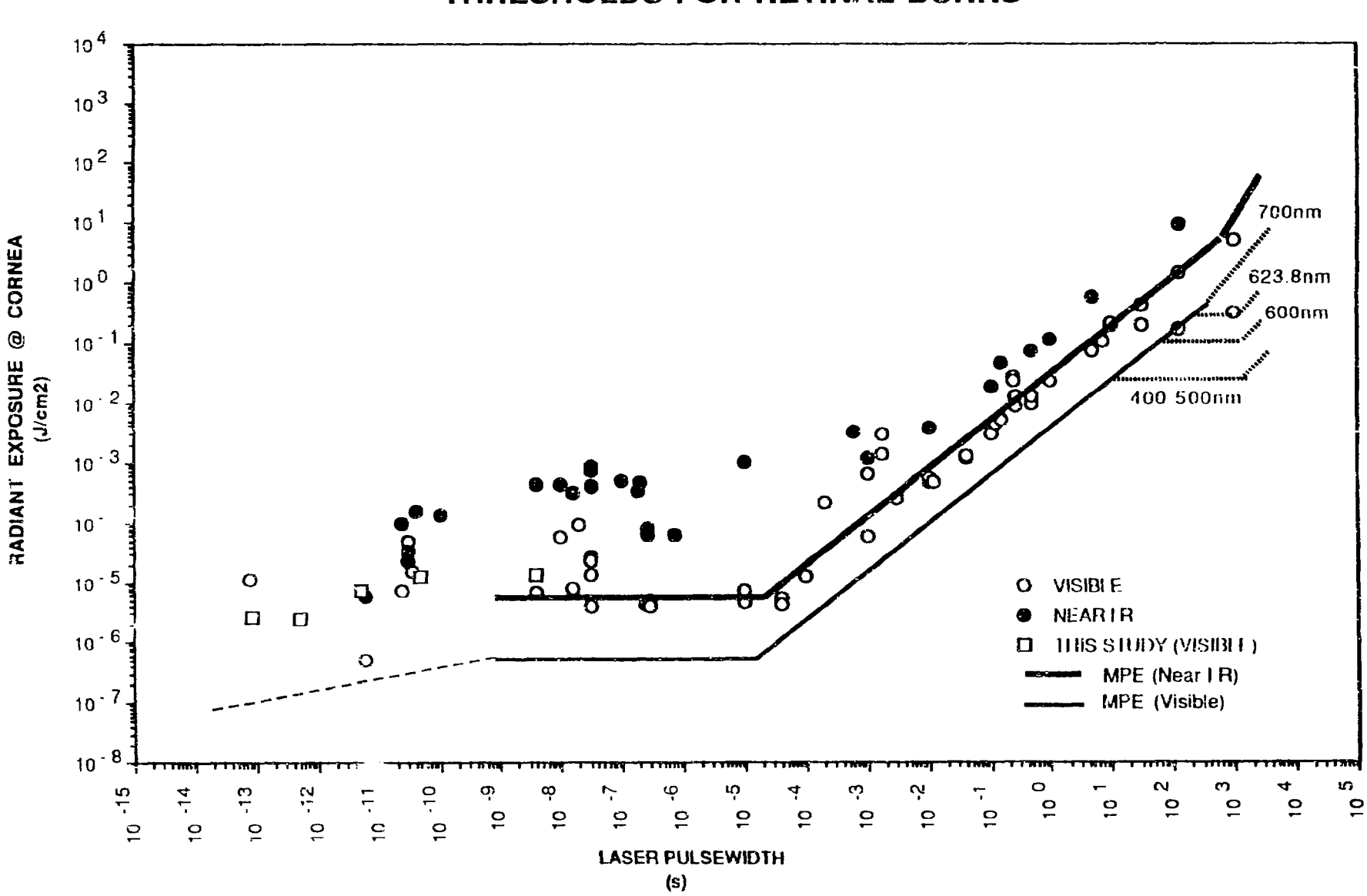

Figure 15. Experimental ED_{50} retinal damage thresholds plotted on a log-log graph of corneal radiant exposure versus laser pulsewidth. Safety standard MPE levels are indicated by the solid and dotted lines. The dashed line indicates the suggested continuation of the visible MPE curve based upon the data from the current study.

Table 3. Comparison of Exposure Parameters and Results from Current Study with those of Birngruber et al.[5]

	Birngruber et al.	Current Study
Subject	Chinchilla Grey Rabbit	Dutch Belted Rabbit
Pulsewidth	80 fsec	90-100 fsec
Wavelength	625 nm	580 nm
Retinal Image Size	50 μm (controlled)	Diffraction Limited (no controlling optics)
MVL Threshold*	4.5 μJ	~1.0 μJ
Fluorescein Threshold*	0.75 μJ	~1.0 μJ
Hemorrhage Threshold	>100 μJ(?)	>120 μJ(?)
Suprathreshold Lesions	No	Yes

*1-hr postexposure

could account for the quantitative difference in MVL threshold. An additional difference in reported observations is that Birngruber et al. found only lesions of MVL appearance even with exposure doses up to 100 μJ. We found ultimate lesion size to increase with dose; being of the order of 500-μm diameter for 120-μJ exposures. Neither study found hemorrhagic lesions, even with the highest pulse energies available.

Birngruber et al.'s[5] observations caused them to speculate that a "nonlinear mechanism in the laser-tissue interaction process acts to limit the retinal damage produced by femtosecond laser pulses." While we concur with this statement, our negative results on laser-tissue interactions when working with isolated ocular tissues do not demonstrate an interaction effect which modifies the pulse in passing through the ocular media. Rather, we infer that a nonlinear interaction mechanism occurs only at the relatively weakly absorbing anterior retinal layers or just in front of the retina where the focusing of the incoming ultrashort pulse could result in achieving the threshold for optical breakdown. In that case, the geometrical pattern of energy dispersal following the plasma formation and cavitation associated with optical breakdown[8] may be different from that following acoustic or mechanical shock-wave generation resulting from linear absorption at the retinal pigment epithelium (RPE). In particular, we speculate that with optical breakdown in the inner retinal layers or in front of the

retina, there is less forward propagation of energy reaching the choroid than there would be without the laser-induced breakdown. This factor could account for the lack of hemorrhage production with the shorter pulsewidths (especially the 90-fs pulses) since hemorrhage production would require forward propagation of energy from the retinal absorption/ interaction site to the choroidal vessels.

There is little reason to expect that the ophthalmoscopic appearance of damage associated with the optical breakdown process suggested in the preceding paragraph would differ from that observed following lesion production by longer pulses (ps-μs) of equal energy. Indeed, the only subjective difference that we can report is the general impression that suprathreshold exposure to 90-fs pulses yielded lesions that appeared to be raised slightly relative to the RPE layer. This difference could be explained if the optical breakdown threshold with 90-fs pulses was reached slightly in front of the retina. It may be that histopathologic evaluation of damage induced by the various pulsewidths used in this study would provide further clues as to the damage mechanism operative in each case. We are currently awaiting pathologic reports on several rabbit eyes exposed to ultrashort laser pulses.

REFERENCES

1. Zuclich, J.A. Ocular effects of ultrashort-pulsewidth laser radiation. USAF AL Protocol RZV-91-04, May 1991.

2. Cain, C.P. Ultrashort-pulse laser system: theory of operation and operating procedures. AL-TR-1991-0146, 1991.

3. ANSI Standard Z136.1-1986. American national standard for the safe use of lasers. American National Standards Institute, Inc., New York, 1986.

4. AFOSH Standard 161-10. Health hazards control for laser radiation. Dept. of the Air Force, Washington, D.C., 1980.

5. Birngruber, R., C.A. Puliafito, A. Garvande, W. Lin, R.W. Schoenlein, and J.G. Fujimoto. IEEE J Quan Elec QE-23:1836-1844 (1987).

6. Allen, R.G., S.J. Thomas, R.F. Harrison, J.A. Zuclich, and M.F. Blankenstein. Ocular effects of pulsed Nd laser radiation: variation of threshold with pulsewidth. Health Phys 49:685-692 (1985).

7. Hochheimer, B.F. Second harmonic light generation in the rabbit cornea. Appl Optics 21:1516-1518 (1982).

8. Zysset, B., J.G. Fujimoto, and T.F. Deutsch. Time-resolved measurements of picosecond optical breakdown. Appl Phys B48:139-147 (1989).

Notes added in proof: In a later experiment using a hyperopic rabbit eye, retinal hemorrhages were induced by 90-fs pulses with pulse energies as low as 30 μJ. Also in a later experiment, additional 5-ps exposures were carried out so that the ED_{50} threshold from probit analysis could be determined with 95% confidence intervals. The amended MVL threshold with 95% confidence limits is 2.6 μJ (2.3 - 2.9 μJ).